

Supplementary Information

Visible light sensitized near-infrared luminescence of ytterbium via ILCT states in quadruple-stranded helicates

Zihan Zhang, Yanyan Zhou, Hongfeng Li,* Ting Gao and Pengfei Yan*

Key Laboratory of Functional Inorganic Material Chemistry, Ministry of Education, P. R. China;
School of Chemistry and Materials Science, Heilongjiang University, Harbin 150080, P. R. China.

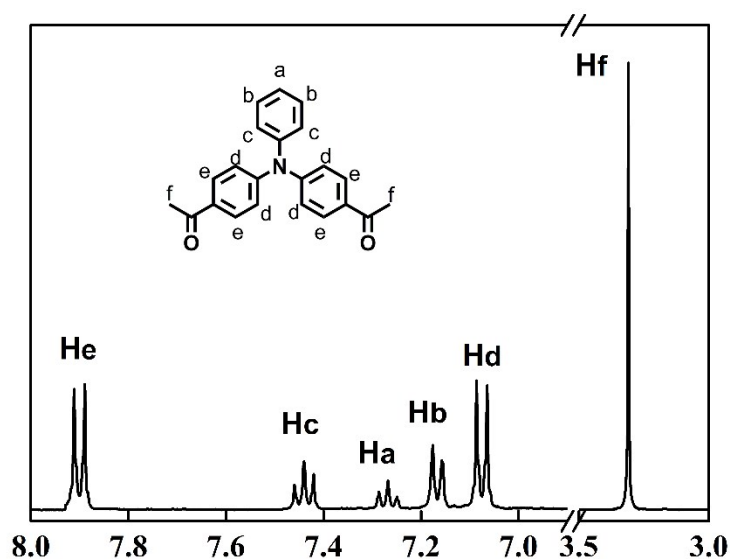


Figure S1. ¹H NMR spectrum of 4,4'-diacetyl triphenylamine in DMSO-*d*₆.

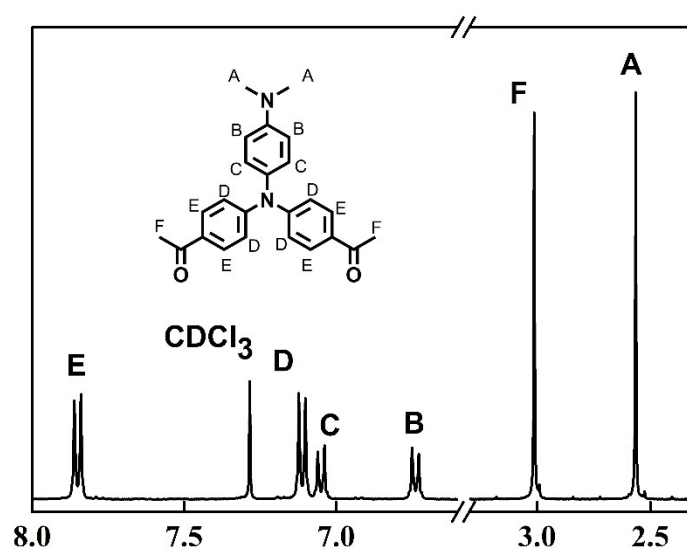


Figure S2. ¹H NMR spectrum of 4-(N,N-Dimethylamino)-4',4''-diacetyltriphenylamine in CDCl₃.

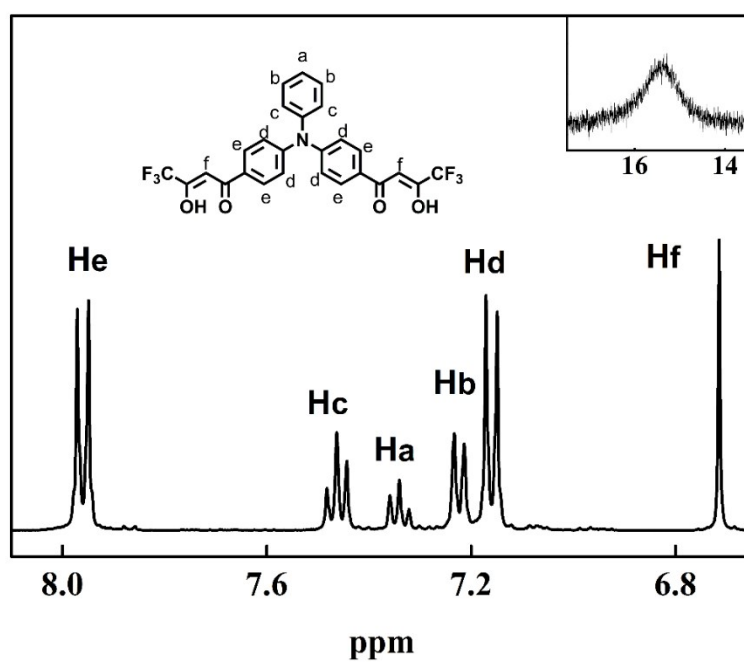


Figure S3. ¹H NMR spectrum of **L¹** in DMSO-*d*₆.

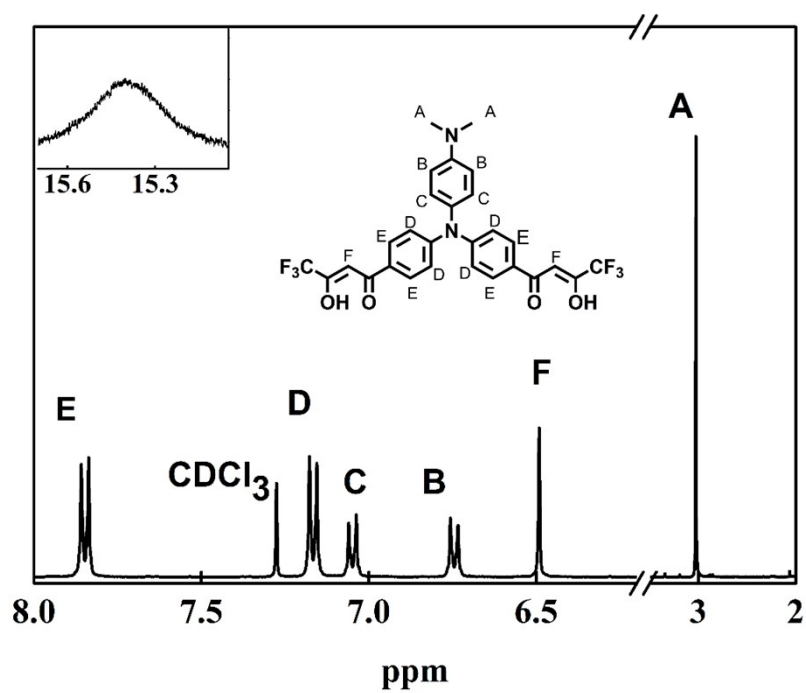


Figure S4. ¹H NMR spectrum of **L²** in CDCl₃.

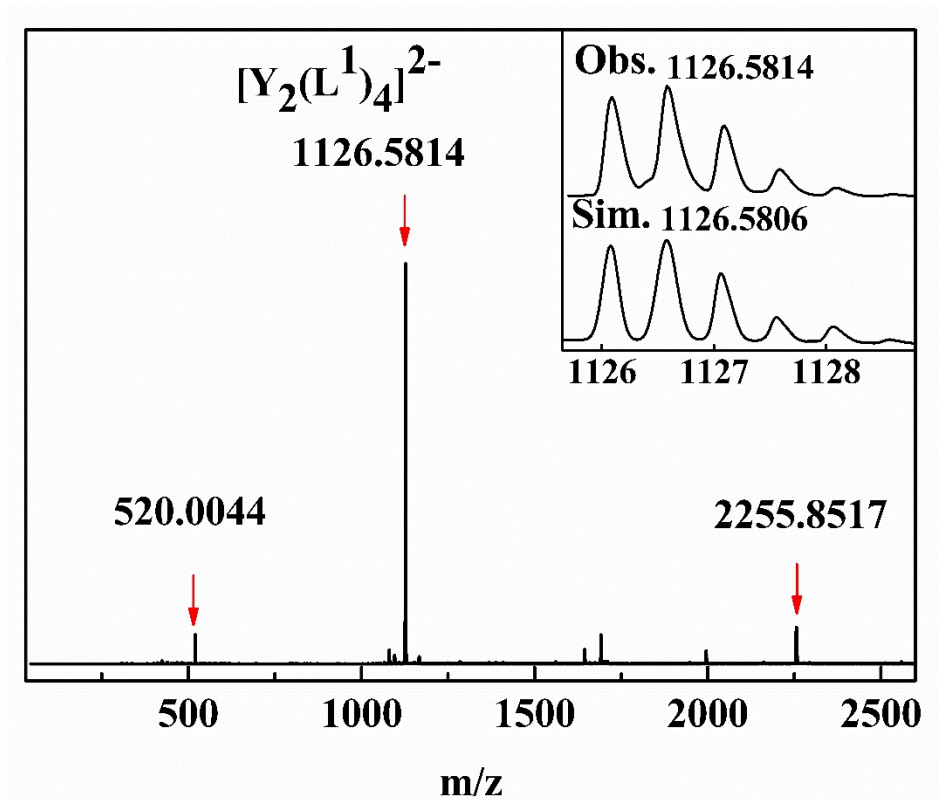


Figure S5. ESI-TOF-MS of $[Y_2(L^1)_4]$.

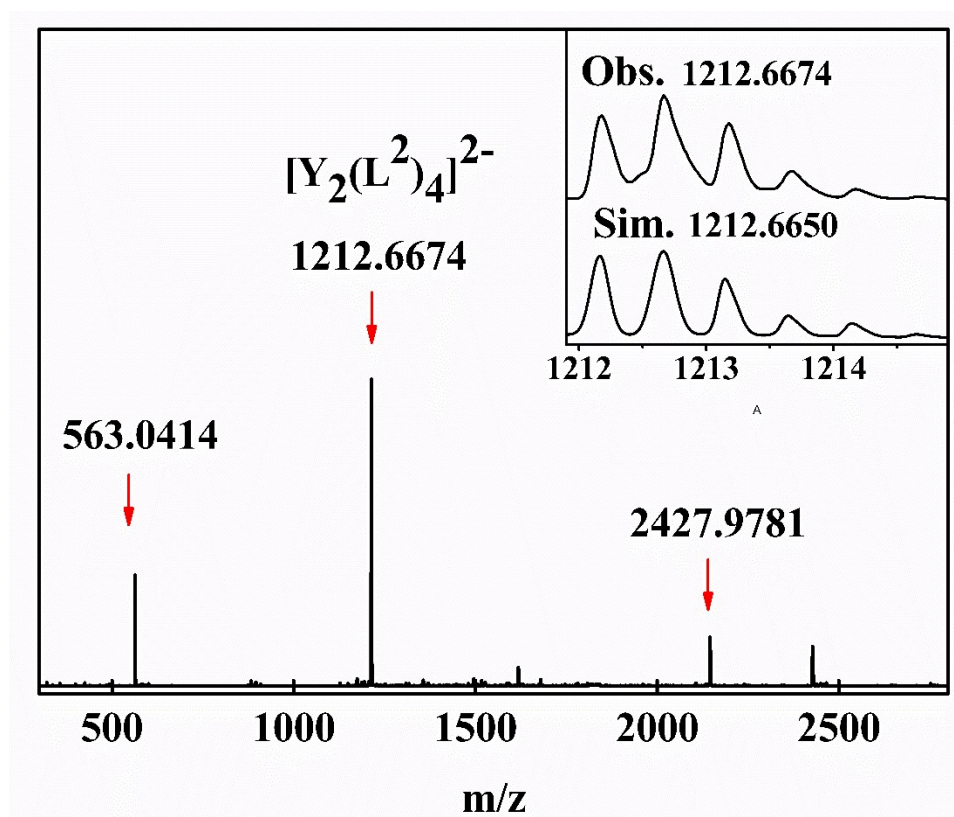


Figure S6. ESI-TOF-MS of $[Y_2(L^2)_4]$.

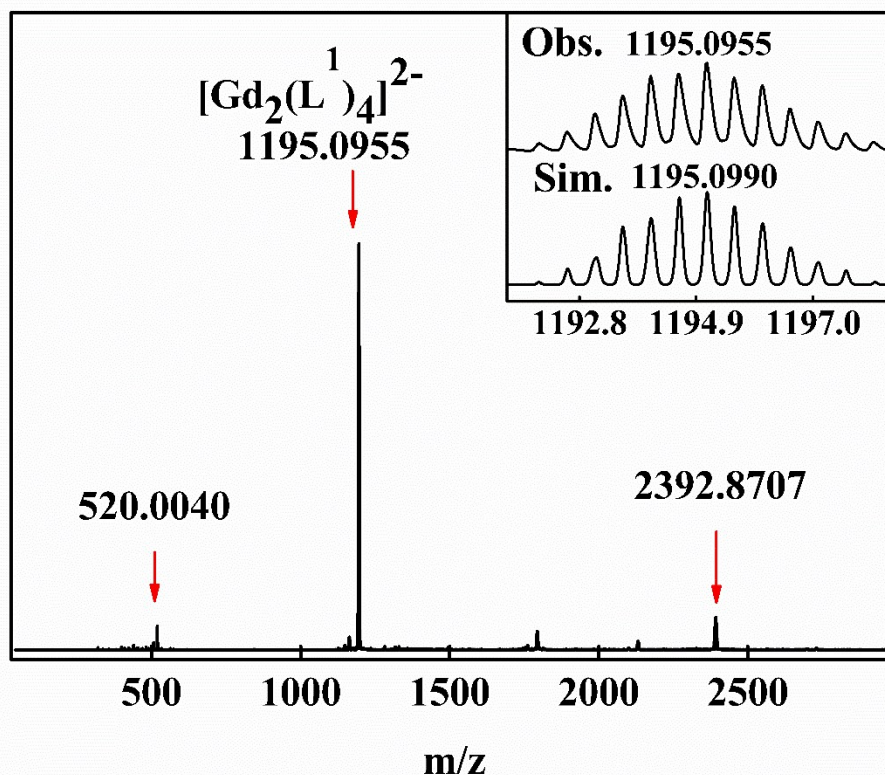


Figure S7. ESI-TOF-MS of $[\text{Gd}_2(\text{L}^1)_4]$.

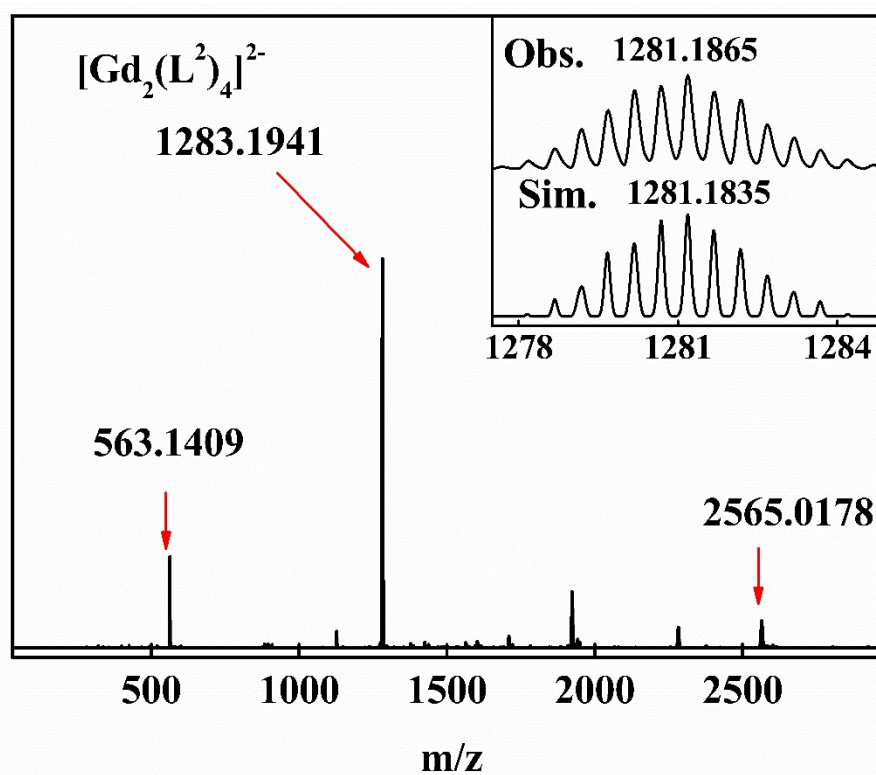


Figure S8. ESI-TOF-MS of $[\text{Gd}_2(\text{L}^2)_4]$.

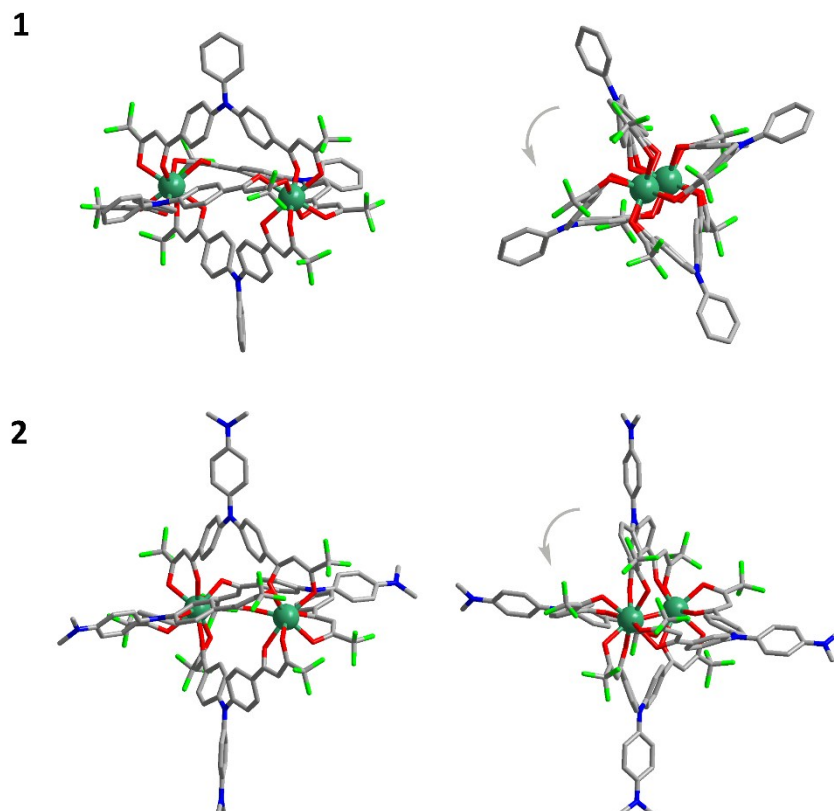


Figure S9. Side view (left) and top view (right) of the structures of complexes **1** and **2** optimized by Sparkle/PM6 model (For clearance, only right-handed Δ - Δ helix are presented).

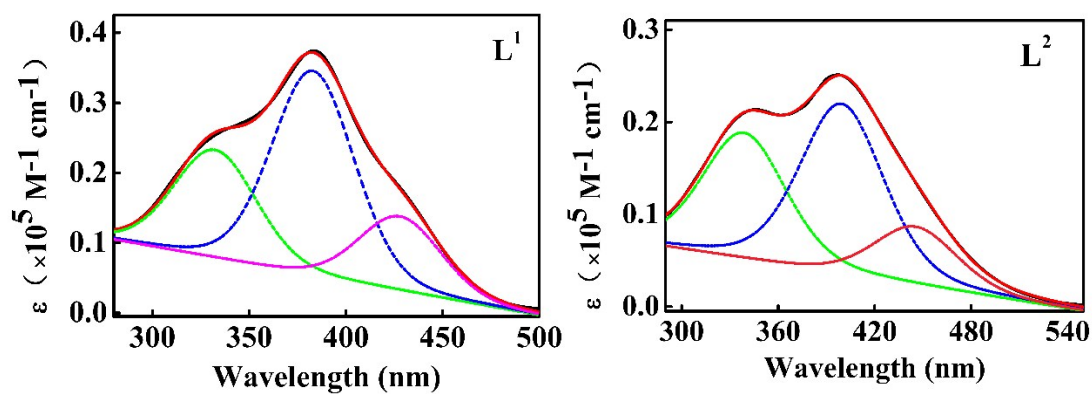


Figure S10. Experimental UV/Vis absorption spectra (solid black line), respective Gaussian deconvolutions (dashed lines), and best fit (solid red line): $R=0.9995$ (for **L**¹), and $R=0.9999$ (for **L**²).

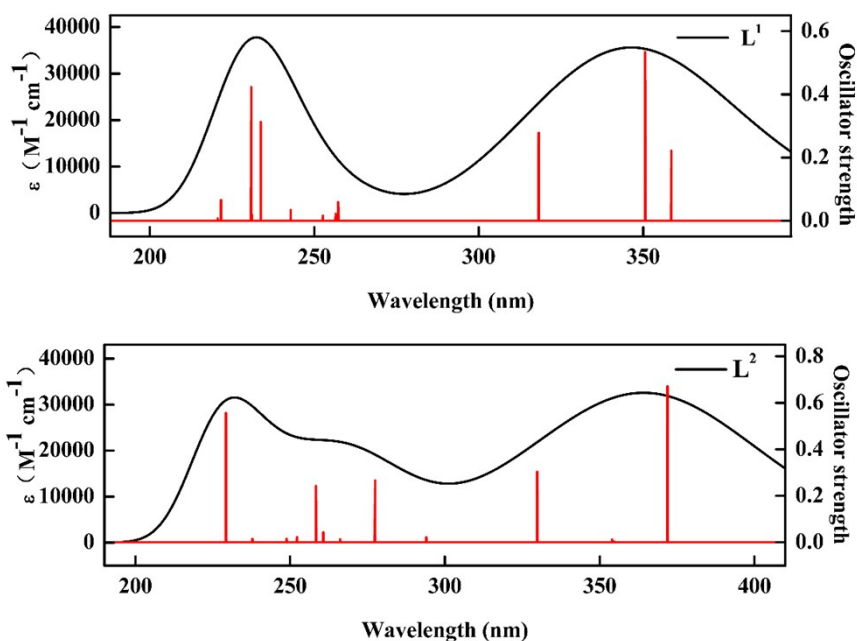


Figure S11. Theoretical UV-Visible absorption spectra of L^1 (up) and L^2 (down) and selected most pertinent lowlying electronic transitions and assignment of L^1 , L^2 .

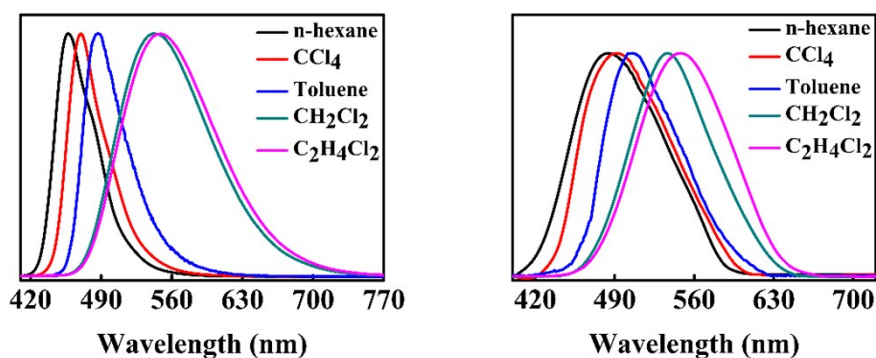


Figure S12. Normalized emission spectra of L^1 and L^2 in various solvents.

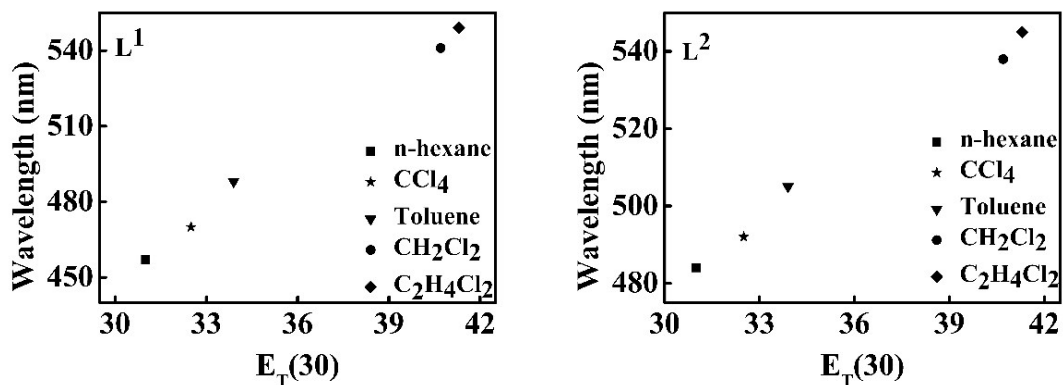


Figure S13. Variation of the emission wavelength maximum for L^1 and L^2 as a function of Reichardt's empirical solvent polarity parameters $E_T(30)$.

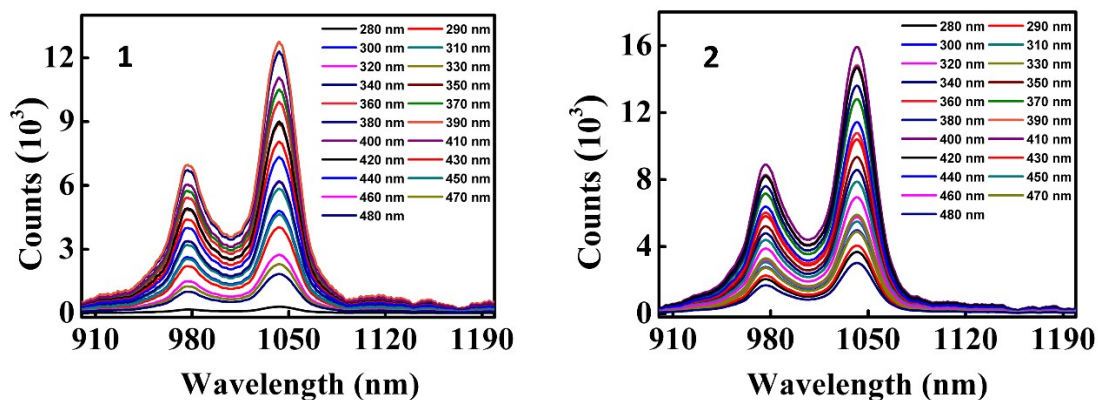


Figure S14. Wavelength dependent emission spectra of complexes **1** and **2**.

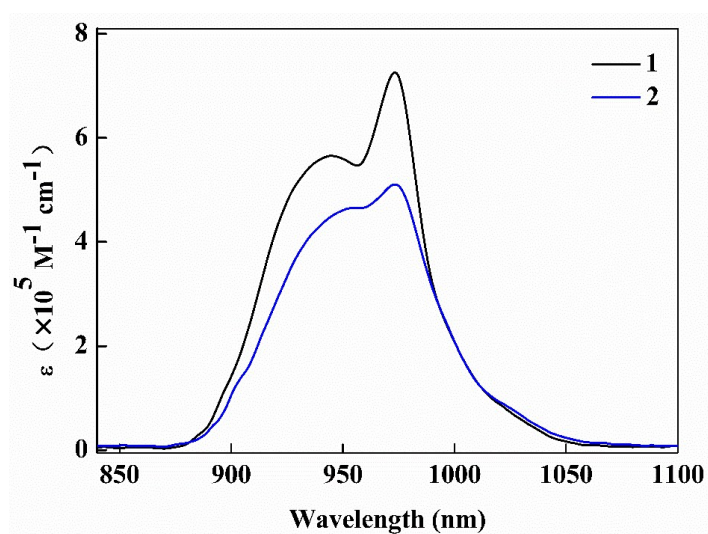


Figure S15. Near-infrared spectra of f-f absorption transition for **1** and **2** in CH₃CN.

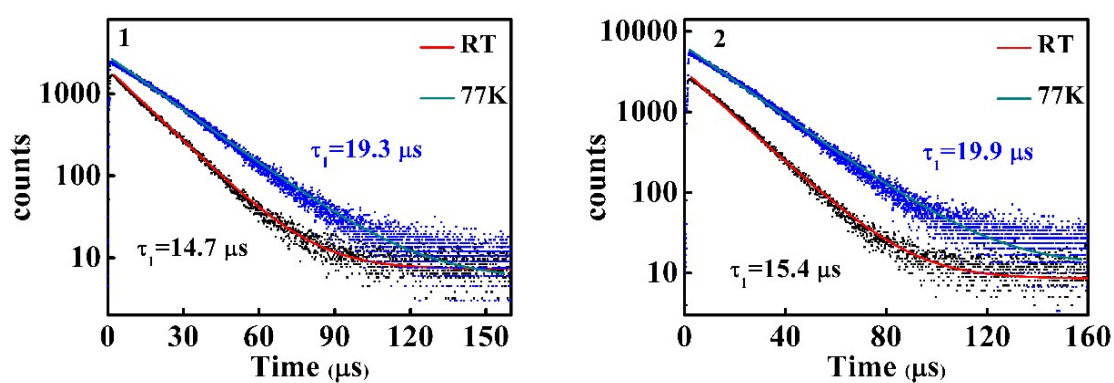


Figure S16. Luminescence decay curves of **1** and **2** in CH₃CN monitored at 1042 nm.

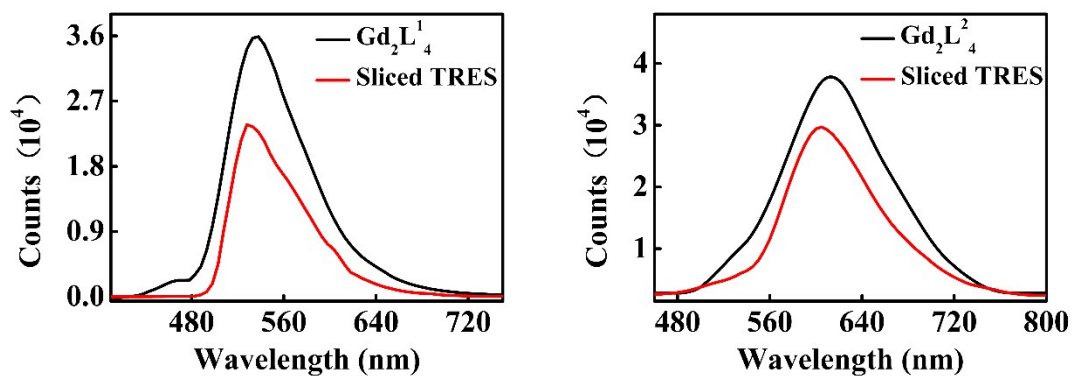


Figure S17. Emission spectra of Gd_2L_4 (black) at 77 K and time delay (100 μs) in CH_3CN .

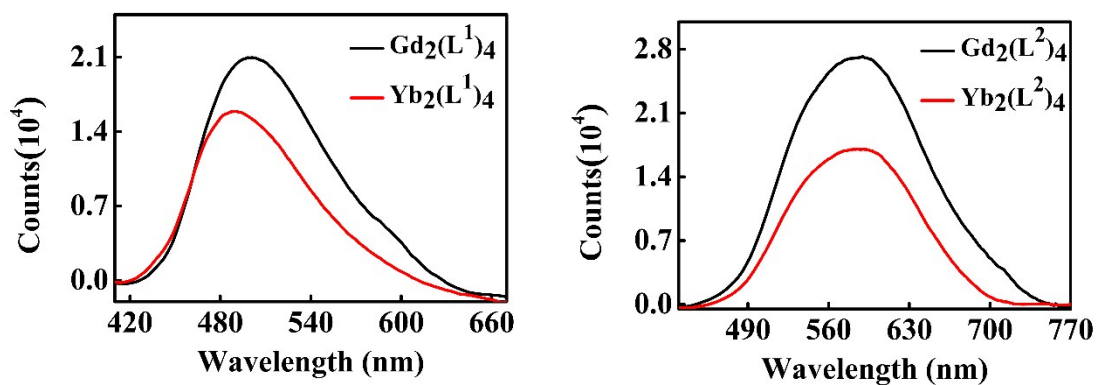


Figure S18. Emission spectra of Gd_2L_4 (black) and Yb_2L_4 (red) in CH_3CN at room temperature.